Journal of Tropical Forest Science 29(3): 267–274 (2017)
https://doi.org/10.26525/jtfs2017.29.3.267274

NEIGHBOURHOOD OF VESSELS: CHEMICAL COMPOSITION AND MICROFIBRIL ANGLE OF FIBRE WITHIN *ACACIA MANGIUM*

R Yahya[1, 3, *], Yansen[1], A Sundaryono[2], Y Horikawa[3, 4] & J Sugiyama[3]

[1]*Faculty of Agriculture, University of Bengkulu, Kota Bengkulu 38371.A, Indonesia*
[2]*Graduate School of Science Education, University of Bengkulu, Kota Bengkulu 38371.A, Indonesia*
[3]*Research Institute for Sustainable Humanosphere, Kyoto University, Uji, Kyoto 611-0011, Japan*
[4]*Faculty of Agriculture, Tokyo University of Agriculture and Technology, Fuchu, Tokyo 183-8509, Japan*

**ridwanyahya@unib.ac.id*

Submitted March 2016; accepted October 2016

Fibre length is affected by vessel transverse enlargement during differentiation, following derivation from fusiform initial cells. In previous studies, thicker and shorter fibres were found adjacent to vessel. The objective of this study is to investigate the chemical composition and microfibril angle (MFA) of fibres, depending on their distance from vessel. A wood block of 10 × 7 × 7 mm (R × T × L) was sliced into 5 µm and 20 µm thickness in a radial-longitudinal direction, as samples for chemical composition and MFA analysis, respectively. The distance of fibres from the vessel was used as the parameter to classify the fibres into two groups. Fourier transform infrared (FTIR) combined with principal component analysis (PCA) demonstrated that higher lignin and lower carbohydrate content were attained from fibres adjacent to vessel, compared to the distant ones. In addition, visualising cellulose microfibril by iodine precipitation technique indicated that MFA of fibre increased with closer distance to vessel. The results obtained in this study would allow us to control the quality of processing for better pulp production.

Keywords: Lignin, carbohydrate, MFA, FTIR spectroscopy, PCA, iodine precipitation technique

INTRODUCTION

A major species in the Indonesian timber estate is *Acacia mangium* (Yamashita et al. 2008, Leksono et al. 2008, Rokeya et al. 2010, Tarigan et al. 2011) which is mainly used for pulp, paper and other wood products (Beadle et al. 2007, Kim et al. 2009, Le Roux et al. 2009, Yong et al. 2011, Asmah et al. 2013). Principal characteristics of wood fibre that influence the yield and paper quality are length, wall thickness, chemical composition and microfibril angle (MFA) (Yahya et al. 2010, Pirralho et al. 2014).

Acacia mangium's vessels occupy 12.1% of the whole wood (Yahya et al. 2010). Fibre length is affected by the vessel transverse enlargement during differentiation, following derivation from fusiform initial cells (Yahya et al. 2011). A 3D dataset of *A. mangium* can be used to give approximate distribution of the length and wall thickness of fibres, in relation to distance from vessels. The fifth and second fibres from the vessel, in radial (RD) and tangential (TD) directions, are substantially shorter than farther ones. The relationship of fibre length and radial vessel distance (r = 0.83) is inversely proportional up to the fifth fibre, and then steady (Yahya et al. 2011). Furthermore, similar patterns of variation of wall thickness and fibre length are acquired up to fifth and second fibre from the vessel in RD and TD (Yahya et al. 2015).

There were no previous studies reported on the chemical composition and MFA as a function of distance from vessel. This is due to the difficulty in gaining information on the approximation of length and wall thickness, due to cell damage that is caused by maceration technique. The development of fourier transform infrared (FTIR) microscopy, with its non-destructive and rapid technique that surpasses conventional techniques, enabled studies on wood and other lignocellulosics' surface characterisation, as well as lignin and carbohydrate content evaluation. The conventional method is laborious and destructive to natural polymer (Pandey 1999).

The application of FTIR spectroscopy technique provides qualitative results. The spectroscopic data, together with multivariate analysis, facilitate the screening of inferior samples from large datasets and associated factor analysis, used to analyse wood samples. The utilisation of microscopy and spectroscopy techniques, concurrently, facilitate the assessment of regions of a sample as small as 50 µm × 50 µm (Chen et al. 2010). Microfibril orientation using brightfield microscopy is pictured by employing iodine precipitation technique, i.e. by precipitating iodine crystals within the cell wall (Donaldson 2008, Ansell 2011, Ishiguri et al. 2012). The objective of the study was to investigate the chemical compositions and MFA of fibres, adjacent to and distant from the vessel using FTIR microscopy and iodine precipitation technique.

MATERIALS AND METHODS

A wood block of 10 × 7 × 7 mm (in radial, tangential and longitudinal directions) (R × T × L) was sliced into 5 µm and 20 µm in thickness in a radial-longitudinal direction, as samples for chemical composition and MFA analysis. The distance of fibres from the vessel was used as the parameter to classify the fibres into two groups based on a previous report, i.e. fibres adjacent to vessel and fibres distant from vessel (Yahya et al. 2011). The first group compromises of fibres located at a distance of up to the fifth and second cell from the vessels in RD and TD directions, respectively, while the second group are fibres located further away from the vessels (Figure 1).

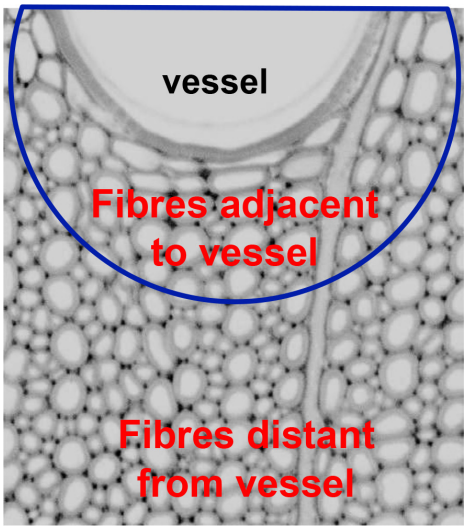

Figure 1 Groups of fibre based on their distance from vessel

For chemical composition analysis, FTIR spectral measurement was carried out using a spectrometer, with an auto image microscope accessory equipped with a low-noise detector (HgCdTe). The samples were set in a sample holder and spectra was recorded with a spectral resolution of 4 cm^{-1} and acquisition of 128 scans in a transmission mode. Spectra for fibres, adjacent to and distant from vessels, were obtained from 10 and 8 regions of interest (ROI), 75 µm × 75 µm, respectively. The Savitzky-Golay algorithm was used to transfer the original spectra to the second derivative spectra, followed by multivariate analysis (Serafińczuk et al. 2011). Since precise characterisation of the wood spectral data is not easy to accomplish due to overlapping bands of hemicelluloses, cellulose and lignin, the spectra was processed with principal component analysis (PCA) to improve interpretation of the spectral data (Al-Qadiri et al. 2008, Chen et al. 2010, Lee et al. 2010). The commercially available software (Unscrambler® *v.9.8*, CAMO Software, Inc. Woodbridge, New Jersey) was used to complete the PCA.

For MFA analysis of fibres, Schultze mixture with 6 g of $KClO_3$ and 100 mL of 35% HNO_3 was made. The sample sections were then soaked in a solution of H_2O:Schultzes mixture, 2:1, for 3 days, followed by direct staining on the glass slide and blotting with 3% iodine-potassium iodide for 3–5 seconds. Filter paper was used to remove the excess solution. Two drops of ice cooled 60% HNO_3 were put on the section under ventilation, mounted by a cover slip. The picture of MFA of S_2 layers was then immediately taken using a microscope with digital camera. Finally, the MFA of 30 fibres adjacent and 30 fibres distant from vessel were analysed using an image analysis software (Image J ver.1.42q Wayne Rasband, National Institute of Health, USA) (Figure 2).

RESULTS AND DISCUSSION

Chemical composition

To understand the variation of chemical components of fibres, depending on the distance from the vessel, PCA based on FTIR spectra was performed in the region of 1550–1200 cm^{-1} (Figure 3) and 1200–800 cm^{-1} (Figure 4), the latter termed as 'finger print'. Figure 3a and b show the original and second derivative spectra, 1550–1200 cm^{-1}, respectively. The PCA

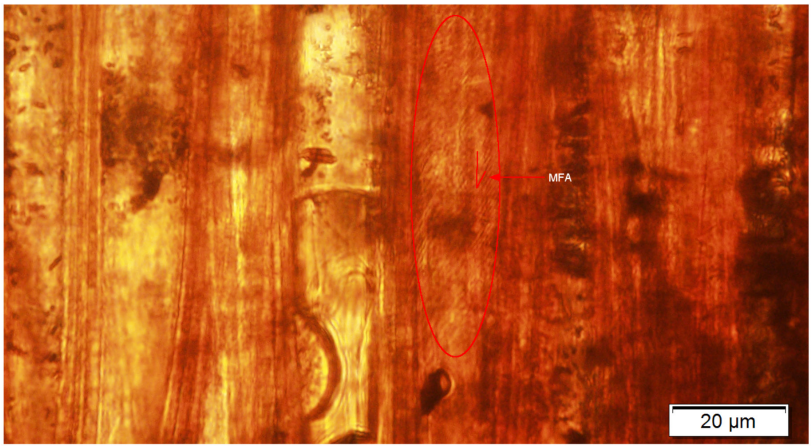

Figure 2 MFA measurement with the indication of precipitating iodine crystals

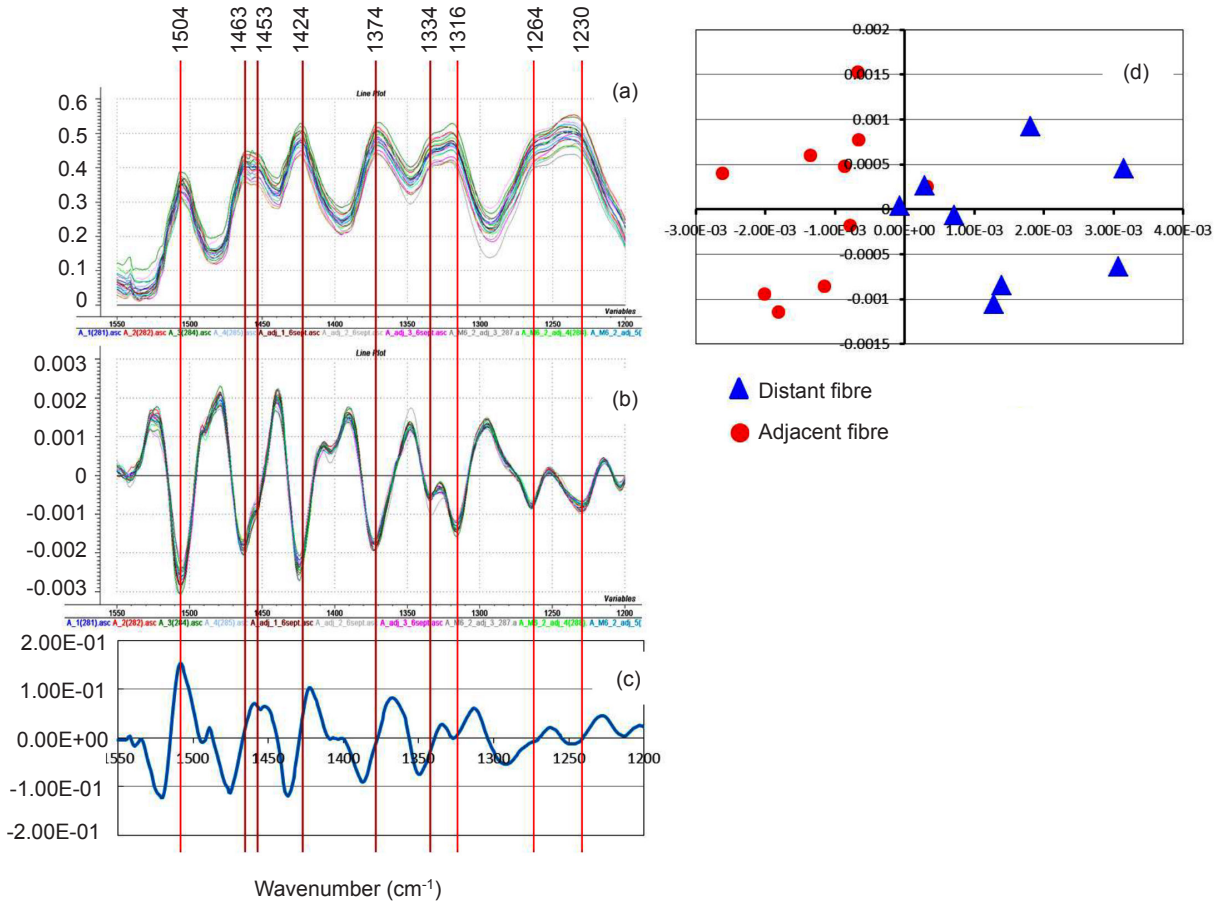

Figure 3 (a) original spectra in the range of 1550–1200 cm^{-1}, (b) secondary derivative spectra, (c) PC1 loading and (d) PCA score plots for fibres in relation to their distance from the vessel

score plots using second derivative spectra was clearly classified according to PC1 axis, as shown in Figure 3d, where distant fibres localised on the right side while those adjacent to the vessel shifted to the left. In order to find the key components separating adjacent fibres from distant ones, the loading vector from PC1 was calculated in the corresponding region (Figure 3c). PC1 loading showed a noticeable positive band at 1504 cm^{-1} which was assigned to the aromatic skeleton from lignin, similar as reported by Pandey (1999) (Table 1). The lignin content can be estimated from the relative area of the 1505 cm^{-1} band, since a linear relationship is

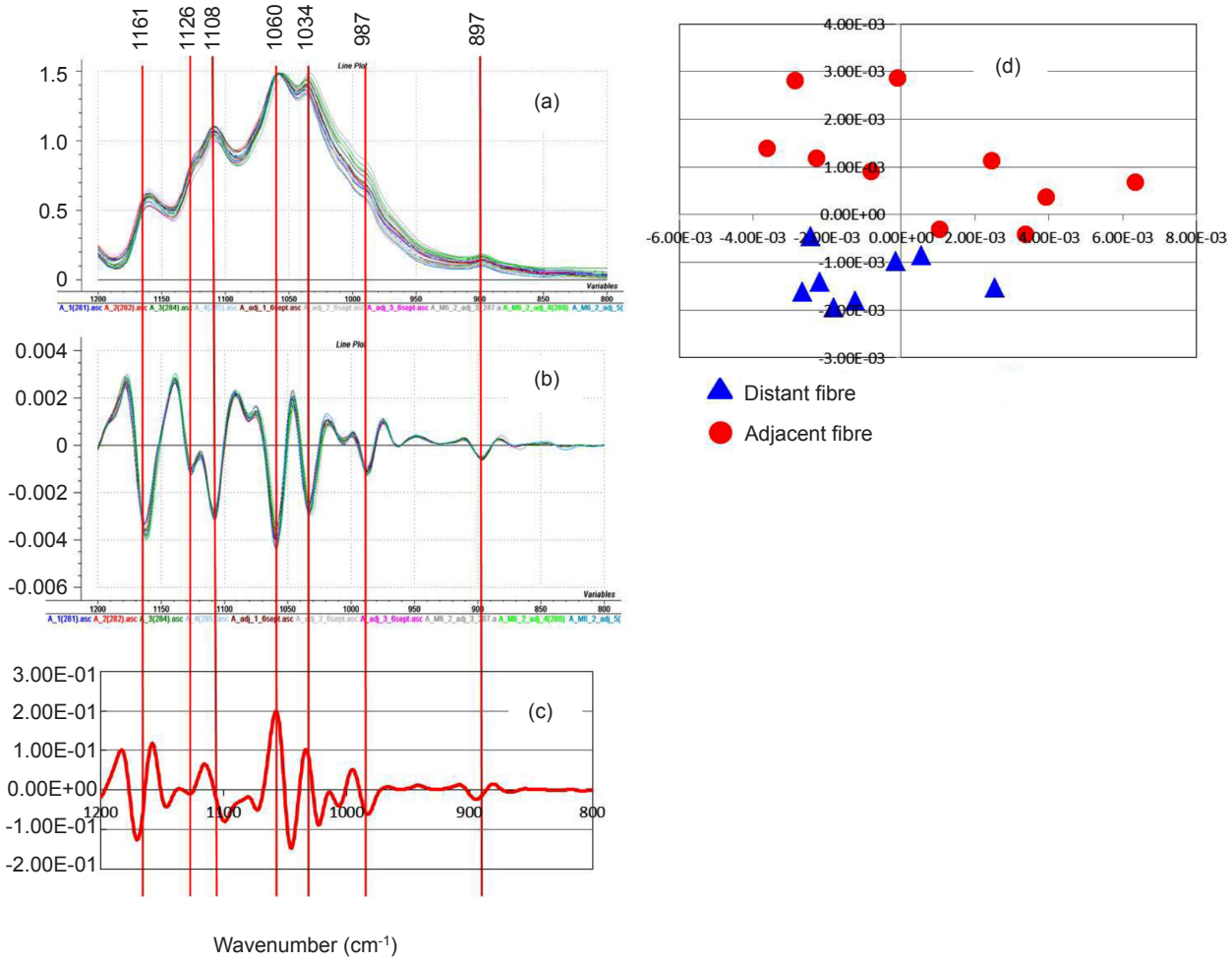

Figure 4 (a) original spectra 1200–800 cm^{-1}, (b) secondary derivate spectra, (c) PC2 loading spectrum and (d) PCA score plots for fibres in relation to their distance from the vessel

Table 1 The FTIR bands used for analysis and their assignment to lignin (Pandey 1999)

Band position (cm^{-1})	Assiginment	Structural component
1504	Aromatic skeletal vibration	lignin
1463	C–H deformation	hemicellulose, lignin
1453	C–H deformation	hemicellulose, lignin
1424	O–H in-plane deformation	cellulose
	COO– stretch aromatic skeletal vibration	hemicellulose, lignin lignin
1374	C–H deformation	cellulose, hemicellulose
1334	C–H in–plane deformation	cellulose, hemicellulose
1316	C–H in–plane deformation	cellulose, hemicellulose
1264	C–O guaiacyl ring	lignin
1230	C–O guaiacyl ring	lignin

found to exist between its area and lignin content (Popescu et al. 2011, Hauptmann el al. 2013, Jiraprasertwong et al. 2014, Avram et al. 2015). Since PCA was conducted by applying second derivative spectra (Figure 3b), the positive band specific to aromatic framework vibration in loading vector suggested that higher quantities of lignin were accumulated in the fibre region adjacent to the vessel rather than distant from the vessel.

Figure 4a and b show the original and second derivative spectra in the range 1200–800 cm^{-1}, where stretching vibrations of C–O, C–C, ring structures and deformation vibrations of CH_2 groups are involved (Synytsya et al. 2010). It has been reported that the corresponding region is useful for identification of polysaccharides, and therefore PCA was employed to make score plots which showed clear distinction between fibres adjacent and distant to vessel, along the PC2 axis (Figure 4d). Bands from 950–1200 cm^{-1} are mainly carbohydrates (Bui et al. 2015). The PC2 loading exhibited strong positive signals at 1060 and 1034 cm^{-1} (Figure 4c), the bands of which are specific to C–O stretching vibrations related to polysaccharides (Pandey 1999, Gierlinger et al. 2008), whose assignments on carbohydrate are summarised in Table 2. Score plots and PC2 loading, obtained from the finger print region, demonstrated that fibres located close to the vessel tended to have less sugars compared to those distant from the vessel.

Comparison of fibre length and chemical contents, estimated by FTIR spectra, showed that adjacent fibres were shorter, with higher relative lignin content (lignin height/CH height) and lower relative carbohydrates (C-O height/CH height), compared to distant fibres (Figure 5). T-test was preformed to study the difference in lignin and carbohydrate contents between fibres, adjacent and distant from vessel, based on values of transmittance spectra (n = 15). The mean of lignin content for fibres adjacent and distant from vessel were 0.141 and 0.124, respecively, while for carbohydrate content were 0.547 and 0.600, respectively. Statisically, the two groups of lignin and carbohydrate contents were significantly different. The results are in line with a previous study (Yahya et al. 2010), showing that fibre length is negatively correlated with lignin content (r = –0.70) and positively correlated with holocellulose (r = 0.92).

Variation of MFA

Measurement of MFA by iodine technique showed a variation of 21.9°–47.1° in distant fibres, while the values for adjacent fibres had a range of 64.0°–78.0°. Distribution of MFA of fibres, depending on their distance from the vessels, is shown in Figure 6. The average of the MFA fibres, adjacent and distant from the vessel, were 69.6° and 32.0°, respectively. Tabet & Aziz (2010) reported that MFA of *A. mangium* at 90 mm distance from pith is 30.6°, assuming that the position of fibres measured were those apart from the vessel. The MFA results supported a previous study that reported the effect of the presence and quantity of vessels in hardwoods, on MFA (Bonham & Barnett 2001). The results are in line with previously reported data on the negative relationship between MFA and fibre

Table 2 The FTIR bands used for the analysis and their assignment to carbohydrate component (Pandey 1999, Gierlinger et al. 2008)

Band position (cm^{-1})	Assiginment	Structural component
1161	C_4–O–C_1 asymmetric vibration	cellulose, hemicellulose
1126	C–O stretch from polysaccharide and C–H deformation of aromatic ring	cellulose, hemicellulose lignin
1108	Glucose ring stretch	cellulose, hemicellulose
1060	C–O stretch	cellulose, hemicellulose
1034	C–O stretch	cellulose, hemicellulose
987	C–O stretch	cellulose, hemicellulose
897	C_1–H deformation	cellulose, hemicellulose

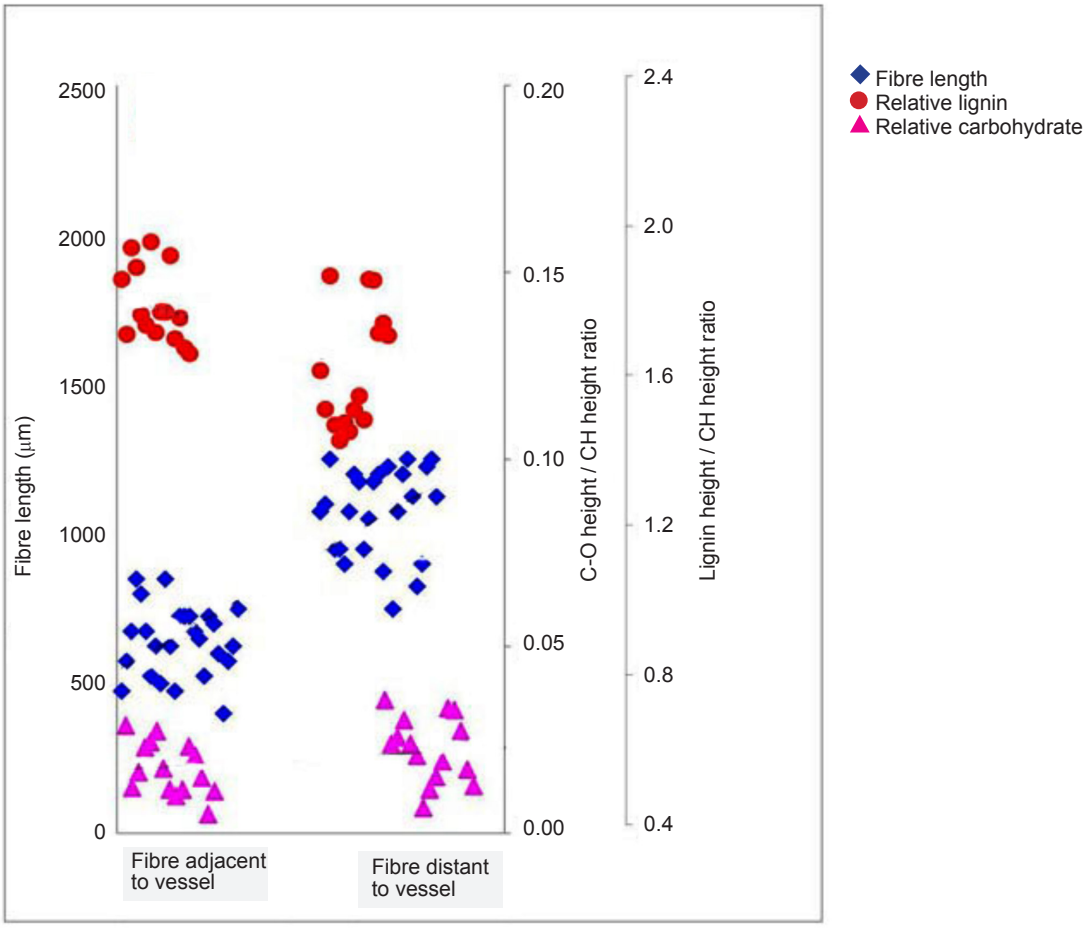

Figure 5 Comparison of fibre length, lignin height/CH height ratio and C–O height/CH height ratio in fibres according to distance from the vessel

Table 3 Comparison of chemical composition in relation to distance from vessels based on value of transmittance spectra

Variables	Adjacent to vessel		Distant to vessel		Significant difference
	Average	SD	Average	SD	
Lignin height/CH height	0.141	0.0098	0.124	0.0157	**
C-O/CH height	0.547	0.0706	0.600	0.0869	**

Note: significant at 1% level, SD = standard deviation

length (Preston 1934). The results also confirm previous data, showing that fibres close to vessels are shorter than those futher away (Yahya et al. 2011).

CONCLUSIONS

The combined FTIR with multivariate analysis succesfully determined the chemical composition of fibre, based on their distance from vessels. Higher lignin and lower carbohydrate content were attained from fibres adjacent to vessel compared to distant ones. For MFA, higher value (69.6°) was gained for fibres adjacent to vessel than the others (32.0°). From the study, it was clear that fibres' distance from vessel affected quality, especially in chemical composition and MFA. Therefore, the utilisation of fibres of wood or other lignocellulosic materials as pulp should take into account the amount of vessels in the feedstock, since more vessels produce lower pulp strength and pulp yield which eventually increase production cost.

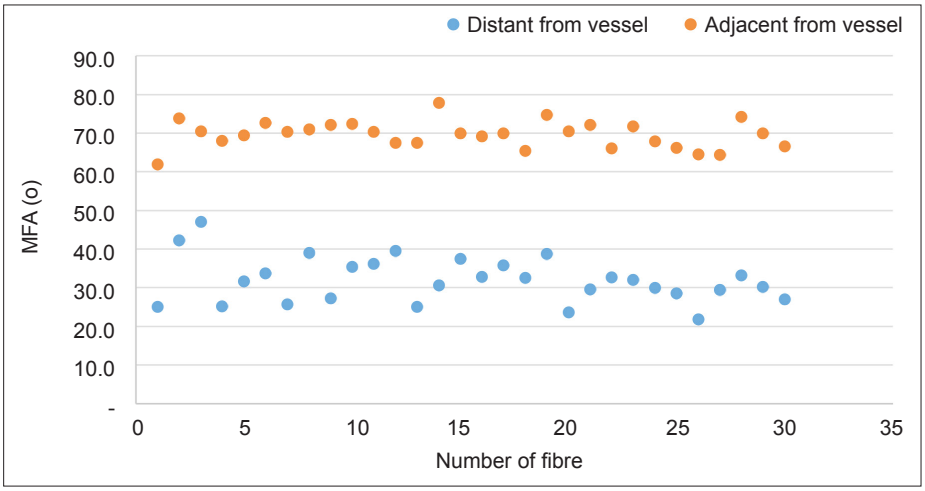

Figure 6 Variation in MFA according to distance from a vessel

ACKNOWLEDGEMENTS

The research was supported by Ministry of Research, Technology and Higher Eduction, Republic of Indonesia. The authors thank and acknowledge Kanai Izumi and Futoshi Ishiguri for their technical assistance in the project.

REFERENCES

Al-Qadiri HM, Al-Alami NI, Al-Holy MA & Rasco BA. 2008. Using fourier transform infrared (FTIR) absorbance spectroscopy and multivariate analysis to study the effect of chlorine-induced bacterial injury in water. *Journal of Agricultural and Food Chemistry* 56: 8992–8997.

Ansell MP. 2011. Wood—a 45th anniversary review of JMS papers. Part 1: The wood cell wall and mechanical properties. *Journal of Mater Science* 46: 7357–7368.

Asmah HN, Hasnida HN, Zaimah NN, Noraliza A & Salmi NN. 2013. Synthetic seed technology for encapsulation and regrowth of *in vitro*-derived Acacia hyrid shoot and axillary buds. *African Journal of Biotechnology* 10: 7820–7824.

Avram A, Covlea V, Matei A, Bazavan M, Butoi B, Bita B & Jipa A. 2015. Impact of RF and DC plasma on wood structure. *Romanian Reports in Physics* 67: 1028–1039.

Beadle C, Barry K, Hardiyanto E, Irianto R, Junarto Mohammed C & Rimbawanto A. 2007. Effect of pruning *Acacia mangium* on growth, form and heart rot. *Forest Ecology and Management* 238: 261–267.

Bonham VA & Barnett JR. 2001. Fibre length and microfibril angle in Silver Birch (*Betula pendula* Roth). *Holzforschung*. 55: 159–162.

Bui Nq, Fongarland P, Rataboul F, Dartiguelongue C, Charon N, Vallée C & Essayem N. 2015. FTIR as a simple tool to quantify unconverted lignin from chars in biomass liquefaction process: application to SC ethanol liquefaction of pine wood. *Fuel Processing Technology* 134: 378–386.

Chen H, Ferrari C, Angiuli M, Yao J, Raspi C & Bramanti E. 2010. Qualitative and quantitative analysis of wood samples by fourier transform infrared spectroscopy and multivariate analysis. *Carbohydrate Polymers* 82: 772–778.

Donaldson L. 2008. Microfibril angle: measurement, variation and relationships- a review. *IAWA Journal* 29: 345– 386.

Gierlinger N, Goswami L, Schmidt M et al. 2008. In situ FT-IR microscopic study on enzymatic treatment of poplar wood cross-sections. *Biomacromolecules* 9: 2194–2201.

Hauptmann M, Muller U, Obersriebnig M, Altmutter WG, Beck A & Hansmann C. 2013. The optical appearance of wood related to nanoscale surface roughness. *Bioresources* 8: 4038–4045.

Ishiguri F, Hiraiwa T, Iizuka K et al. 2012. Radial variation in microfibril angle and compression properties of *Paraserianthes falcataria* planted in Indonesia. *IAWA Journal* 33: 15–23.

Jiraprasertwong A, Gulari E & Chavadej S. 2014. Effect of different microbial strains on biological pretreatment of sugarcane bagasse for enzymatic hydrolysis. *International Science Index* 9: 875–879.

Kim NT, Matsumura J, Oda K & Cuong NV. 2009. Possibility of improvement in fundamental properties of wood of acacia hybrids by artificial hybridization. *Journal of Wood Science* 55: 8–12.

Lee CH, Wu TL, Chen YL & Wu JH. 2010. Characteristics and discrimination of five types of woodplastic composites by FTIR spectroscopy combined with principal component analysis. *Holzforschung* 64: 699–704.

Le Roux C, Tentchev D, Prin Y et al. 2009. Bradyrhizobia nodulating the *Acacia mangium* x *A. auriculiformis* interspecific hybrid are specific and differ from those associated with both parental species. *Applied and Environmental Microbiology* 75: 7752–7759.

Leksono B, Kurinobu S & Ide Y. 2008. Realized genetic gains observed in second generation seedling seed orchards of *Eucalyptus pellita* in Indonesia. *Journal of Forest Research* 13: 110–116.

Pandey KK. 1999. A study of chemical structure of soft and hardwood and wood polymers by FTIR spectroscopy. *Journal of Applied Polymer Science* 71:1969–1975.

Pirralho M, Flores D, Sousa VB, Quilhó T, Knapic S & Pereira H. 2014. Evaluation on paper making potential of nine Eucalyptus species based on wood anatomical features. *Industrial Crops and Products* 54: 327–334.

Popescu MC, Popescu CM, Lisa G & Sakata Y. 2011. Evaluation of morphological and chemical aspects of different wood species by spectroscopy and thermal methods. *Journal of Molecular Structure* 988: 65–72.

Preston RD. 1934. The organisation of the walls of conifer tracheids. *Philosophical Transactions* B224: 131–174.

Rokeya UK, Hossain MA, Ali MR & Paul SP. 2010. Physical and mechanical properties of (*Acacia auriculiformis* x *A mangium*) hybrid Acacia. *Journal of Bangladesh Academy of Science* 34: 181–187.

Serafińczuk J, Pietrucha J, Schroeder G & Gotszalk TP. 2011. Thin film thickness determination using x-ray reflectivity and Savitzky-Golay algorithm. *Optica Applicata* 41: 315–322.

Synytsya A, Kim W, Kim S et al. 2010.Structure and antitumour activity of fucoidan isolated from sporophyll of Korean brown seaweed *Undaria pinnatifida. Carbohydrate Polymers* 81: 41–48.

Tabet TA & Aziz FHA. 2010. Estimation of the cellulose microfibril angle in *Acacia mangium* wood using small angle x-ray scattering. *Journal of Agricultural Sciences* 2: 139–148.

Tarigan M, Roux J, Van Wyk M, Tjahjono B & Wingfield MJ. 2011. A new wilt and die-back disease of *Acacia mangium* associated with *Ceratocystis manginecans* and *C. acaciivora* sp. nov. in Indonesia. *South African Journal of Botany* 77: 292–304.

Yahya R, Koze K & Sugiyama J. 2011. Fibre length in relation to the distance from vessels and contact with rays in Acacia mangium. *IAWA Journal* 32: 341–350.

Yahya R, Sugiyama J, Silsia D & Gril J. 2010. Some anatomical features of an acacia hybrid, *A. mangium* and *A. auriculiformis* grown in Indonesia with regard to pulp yield and paper strength. *Journal of Tropical Forest Science* 22: 343–351.

Yahya R, Sundaryono A, Imai T & Sugiyama J. 2015. Distance from vessels changes fibre morphology in *Acacia mangium. IAWA Journal* 36: 36–43.

Yamashita N, Ohta S & Hardjono A. 2008. Soil changes induced by *Acacia mangium* plantation establishment: comparison with secondary forest and *Imperata cylindrica* grassland soils in South Sumatra, Indonesia. *Forest Ecology and Management* 254: 362–370.

Yong S, Choong YC, Cheong CY et al. 2011. Analysis of ESTs generated from inner bark tissue of an *Acacia auriculiformis* x *Acacia mangium* hybrid. *Tree Genetics and Genomes* 7: 143–152.

